Development of a spectrometer using a continuous wave distributed feedback quantum cascade laser operating at room temperature for the simultaneous analysis of N2O and CH4 in the Earth's atmosphere

Lilian Joly, Cédric Robert, Bertrand Parvitte, Valéry Catoire, Georges Durry, Guy Richard, Bernard Nicoullaud, Virginie Zéninari

Development of a spectrometer using a continuous wave distributed feedback quantum cascade laser operating at room temperature for the simultaneous analysis of N_2O and CH_4 in the Earth's atmosphere

Lilian Joly,[1] Claude Robert,[2] Bertrand Parvitte,[1] Valery Catoire,[2] Georges Durry,[1,3] Guy Richard,[4] Bernard Nicoullaud,[4] and Virginie Zéninari[1,*]

[1]Groupe de Spectrométrie Moléculaire et Atmosphérique, UMR CNRS 6089, UFR Sciences Exactes et Naturelles, Moulin de la Housse, BP 1039, 51687 Reims Cedex 2, France

[2]Laboratoire de Physique et Chimie de l'Environnement, UMR CNRS 6115, 3A, Avenue de la Recherche Scientifique, 45071 Orléans Cedex 2, France

[3]Service d'Aéronomie, Route des Gâtines BP 3–91371 Verrières le buisson, France

[4]Institut National de la Recherche Agronomique, UR0272 Unité de Science du Sol d'Orléans—2163 Avenue de la Pomme de Pin–BP 20619–Ardon–45166 Olivet Cedex

*Corresponding author: virginie.zeninari@univ-reims.fr

We report on the development and performance of a gas sensor based on a distributed feedback quantum cascade laser operating in continuous wave at room temperature for simultaneous measurement of nitrous oxide (N_2O) and methane (CH_4) concentrations at ground level. The concentrations of the gases are determined by a long path infrared diode laser absorption spectroscopy. The long-term stability of the instrument is evaluated using the Allan variance technique. A preliminary evaluation of the instrument performance is realized by *in situ* measurements of N_2O and CH_4 concentrations at ground level during 1 day. The sensor has also been applied to study the time response of N_2O concentrations to a fertilizer addition in a soil sample and for the comparison between various types of soils.

1. Introduction

Concentrations of chemical species contributing to global warming, that is, carbon dioxide (CO_2), chlorofluorocarbons (CFCs), methane (CH_4), and nitrous oxide (N_2O) have been rapidly increasing since the industrial revolution period. CO_2 has been believed to be a primary global warming gas. However, though concentrations of other gases are much smaller than that of CO_2, their absorption of Earth's infrared emission are larger than CO_2, and their contributions to global warming are considerably high. The global warming potentials (GWP) of N_2O and CH_4 at 100 years on the horizon are 296 and 23 times larger than that of CO_2, respectively [1]. Worldwide, concentrations of CH_4 have increased by 148% and those of N_2O by 18% compared to the levels in preindustrial times. Globally, the soil–atmosphere exchange of greenhouse gases is thought to contribute roughly 30% and 70% to the annual emissions of CH_4 and N_2O, respectively [2]. Agricultural soils contribute substantially to this budget. N_2O emission occurs due to the use of mineral and organic

fertilizers in agricultural activity, through the activity of micro-organisms, and to the expirations of human beings [3]. The production of N_2O by soils primarily occurs through two biological processes: (1) denitrification, the anaerobic microbial respiration using nitrate and nitrite as electrons acceptors [4] and (2) nitrification, the exothermic oxidation of ammonium to nitrite and nitrate [5]. CH_4 is produced in soils as the end product of the anaerobic decomposition of organic matter. A better understanding of the soil–atmosphere exchange is necessary to control N_2O and CH_4 emissions with new cropping systems.

N_2O and CH_4 emissions are very variable with time and space [6,7] and difficult to measure. Two main methods are available today [8]: (1) the static method that is based on the measurement of gas concentration within closed chambers that are put at the soil surface during a given period (typically 3 h) and (2) the micrometeorological method that is based on the measurement of the gradient of gas concentration in the atmosphere. Both methods require gas concentration measurements that are done either in the laboratory after atmospheric sampling or directly in the field. Available gas analyzers limit the possibility to measure the gas concentration on a wide scale and over a long period while modern atmospheric research on gas exchange between the biosphere and the atmosphere requires sensitive, reliable, and fast response chemical sensors. Therefore, techniques for fast and simultaneously sensitive trace gas measurements based on tunable diode laser absorption spectroscopy have been successfully applied to micrometeorological trace gas flux measurement techniques [9]. Mid-infrared absorption spectrometers have been developed by different teams [10,11] to demonstrate the applicability of quantum cascade lasers (QCLs) for high precision measurements of N_2O and CH_4 in the Earth's atmosphere. They used a thermoelectrically (TE) cooled pulsed QCL, but to have a high spectral resolution continuous wave (cw) is better because the linewidth of the laser is smaller. Infrared laser absorption spectroscopy is an extremely effective tool for the detection of molecular trace gases. The demonstrated sensitivity of this technique ranges from a parts in 10^6 by volume (ppmv) to a parts in 10^{12} by volume (pptv) level depending on the specific gas species. The usefulness of the laser spectroscopy approach is limited by the availability of convenient tunable sources in the region of fundamental vibrational absorption bands.

Atmospheric sciences have awaited the development of single mode tunable laser sources that operate in the mid-infrared region at room temperature (RT). Distributed feedback (DFB) QCLs operating in cw are promising spectroscopic sources because of their single mode operation with a narrow linewidth (few megahertz), high output power ($P > 10$ mW), reliability, and compactness. In the past, this kind of laser worked at a cryogenic temperature, but now QCLs offer the possibility to work at RT [12]. QCL spectroscopy permits identification, detection, quantification, and monitoring of numerous molecular trace gas species, and cw DFB RT QCLs are promising tools for the development of highly compact laser field deployable sensors.

To study gas soil–atmosphere exchanges a sensor for N_2O and CH_4 detection was developed. The first objective is to obtain a sensor operating at ground level with a high temporal resolution (~10–20 Hz) in order to provide flux measurements in conjunction with wind speed determination. Indeed, land use, fertilizer type, fertilizer application, irrigation, soil type, and crop residues were found to have a profound effect on the N_2O emission factor from agricultural soils [13]. Second, we would like to obtain an instrument light enough to be transported and operated on in the field by two people and with energy autonomy to study spatial and temporal variability of fluxes as a function of these parameters. The need for a new development in comparison with commercial instruments is guided by the possibility that the instrument can be controlled entirely by ourselves and evolve in the future for better performances with other species less abundant to be measured and with higher measurement frequency. Another aspect is the longer optical path than those of companies such as Campbell Scientific Inc. or Aerodyne Research Inc., who sell optical cells with a typical path <100 m. At present the performances of our instrument and those of these companies are almost comparable. However there is potential for the improvement of both optical and electronic systems. In particular the high spectral resolution of a cw QCL is well adapted to select the rovibrational lines of species with very low absorption signals among other major absorbing species.

In this paper we first present an experimental setup of the QCL spectrometer. Details of the data processing are described in Section 2. Section 3 describes the laboratory testing of the N_2O and CH_4 sensor. In particular, the detection limit, the precision, and the long-term stability of the instrument evaluated using the Allan variance technique are detailed. Section 4, we discuss preliminary *in situ* measurements achieved with the laser sensor. A set of concentration data over a period of 26 h is recorded to demonstrate the capability of the sensor to detect N_2O and CH_4 concentration variations. The addition of mineral nitrogen (N) to the soil via mineral N fertilizers generally increases the N_2O emission. The sensor has been applied to study the time response of N_2O concentrations to a fertilizer addition in a soil sample. Finally we present the results of N_2O and CH_4 concentrations obtained with six various types of soils.

2. Design of the Quantum Cascade Laser Spectrometer

The measurements are performed at a high resolution using a direct absorption spectrometer with a new generation of QCL. The direct detection

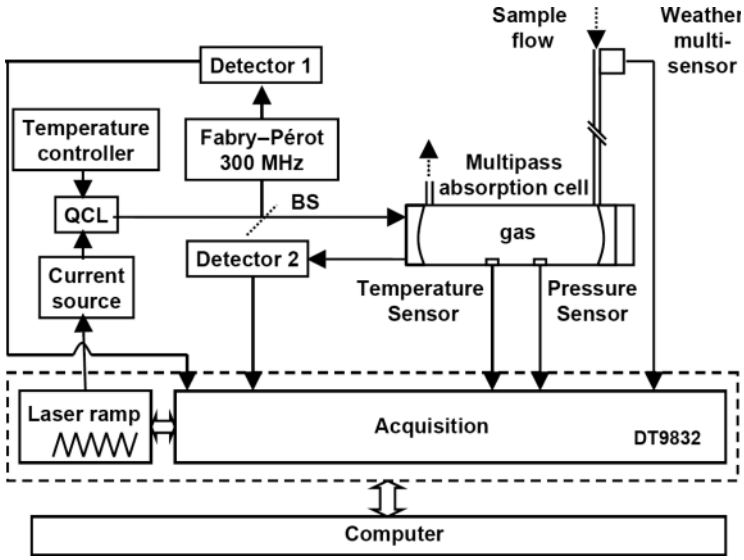

Fig. 1. Experimental setup: QCL stands for quantum cascade laser and BS for beam splitter.

technique is straightforward. A schematic of our optical platform is presented in Fig. 1, and a photograph of the used sensor is depicted in Fig. 2. The QCL from Alpes Lasers (Switzerland) is mounted onto a copper substrate attached to a thermoelectric cooler and contained in a hermetically sealed enclosure (Alpes Lasers LLH). Heat produced by the cooler is removed by circulating water through the base of the enclosure. The QCL operates between −30 °C and +30 °C and the maximum current is 550 mA. The temperature is controlled and stabilized by a model ILX LightWave LDT-5980 high power temperature controller. The current source is an ILX Lightwave model LDX-3232. The tunability range of this laser is from 1265 cm^{-1} (T_{QCL} = −29 °C, I_{QCL} = 550 mA) to 1274 cm^{-1} (T_{QCL} = −29 °C, I_{QCL} = 290 mA). The QCL power is ∼30 mW. The synthetic spectra (Fig. 3) present the QCL's

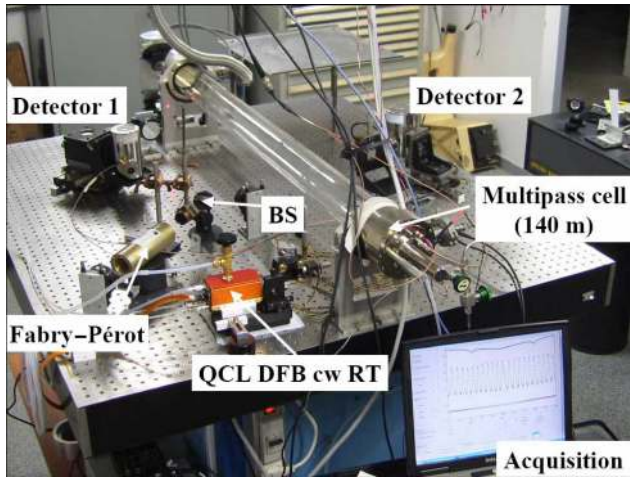

Fig. 2. (Color online) Photograph of the actual sensor.

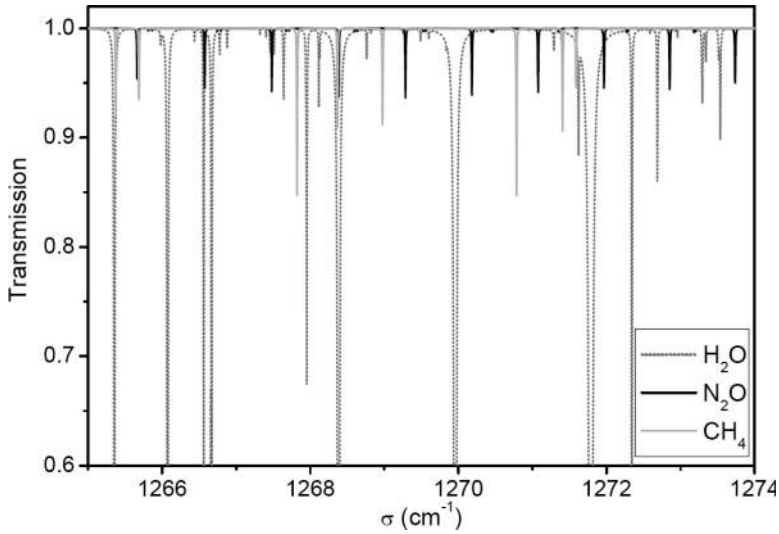

Fig. 3. Calculated spectra using HITRAN 2004 parameters in the QCL's spectral range emission. Temperature is 291 K, pressure is 50 mbar, and path length is 140 m. Volume mixing ratios are 9000 ppm for H_2O, 319 ppb for N_2O, and 2 ppm for CH_4.

spectral range and molecular absorptions. These spectra are calculated using HITRAN 2004 data [14] and show the best spectral window to simultaneously detect N_2O and CH_4. This spectral range is from 1270.7 to 1271.2 cm^{-1}. In this region N_2O and CH_4 lines are isolated enough, and there is no interference with water vapor lines. N_2O and CH_4 lines have intensities of 1.552×10^{-19} cm molecule^{-1} at 1271.07668 cm^{-1} and 5.604×10^{-20} cm molecule^{-1} at 1270.78503 cm^{-1}, respectively [14].

The laser emission wavelength is scanned over the molecular transition by applying a triangular current ramp (100 Hz) to the QCL. The data acquisition is performed by a DataTranslation DT9832 acquisition module. Each spectrum is composed of 1000 points. The measurement signal is the average of 50 successive signal sweeps, and the interval between two acquisitions is 5 s. For flux measurements these conditions may be adapted. At the moment our acquisition system is not sufficiently rapid for this type of measurement but very rapid acquisition cards are now available upon request. The laser beam is collimated by an off-axis parabola (OAP) with a 25.4 mm diameter and a 25.4 mm focal length. A diaphragm on the parallel beam permits adjustment of the beam aperture. The parallel beam is separated into two parts via a beam splitter (BS). The reflected beam is coupled with a Fabry–Pérot (FP) germanium etalon used for relative frequency calibration (free spectral range 0.01 cm^{-1}). The second part of the beam is focused with a spherical mirror ($f = 1$ m) at the entrance of the absorption cell. Both beams are focused by the OAP (from Edmund Optics, F number is 1) on two liquid nitrogen cooled HgCdTe detectors (from French Society Anonyme of Telecommunications; diameter is 500 μm). At the moment liquid N cooled detectors are used, which produce an electric signal in the photovoltaic mode, but in the future it will be possible to use RT detectors.

The optical system is prealigned with a visible diode-laser removed during the measurements. The absorption cell is a new type of multiple-reflection cell presented in [15]. This cell consists of three spherical mirrors as in a White cell, but its principle is different. It behaves as a multiplier of a Herriott cell from which it inherits the optomechanical stability qualities. The Herriott cell and the White cell are two particular cases of this type of cell. One of the main advantages is that it can be made of standard mirrors while allowing a great number of reflections and thus a large optical path. The three mirrors are of equal curvature ($R = 2500$ mm), and the separation between the mirrors is 1.08 m. The mirror coating is protected by gold with an effective reflection coefficient of 98% (much lower than the 99.2% given by the manufacturer). The mirrors are set in a 5 l hermetically sealed housing with two windows (ZnSe Wedge) for the input output beam, an inlet for atmospheric air input, and an outlet for pump ing. Pressure (MKS Baratron) and temperature (PT100) sensors permit measurements of these two important parameters for high resolution spectroscopy. In the configuration used here the optical path is 140 m. The sample gas (outside the laboratory) is brought from atmospheric pressure to ~40 mbar across the inlet orifice to reduce the pressure broadening of the absorption lines, increasing the distinctive nature of the absorbing species spectral signature. The system operates at a gas flow of 5 l/min and the pressure inside is not actively regulated but the drift is only 1.5 mbar per 12 h. The next version of the instrument will benefit from an active pressure control instead of a simple valve. A dust filter is set at the inlet of the measurement head to protect the gas system and the mirrors of the cell from pollution. A WXT510 weather transmitter from Vaisala is used to measure thermodynamic conditions outside the laboratory. It offers six weather parameters: wind speed and direction, liquid precipitation, barometric pressure (accuracy: ±0.5 hPa at 0 °C–30°C), temperature (accuracy at +20 °C: ±0.3 °C), and relative humidity (accuracy 3% within 0%–90%). At the moment, the measurements are limited by the 1 Hz response of the Vaisala system, but in the future it will be possible to use a sonic anemometer with an acquisition rate of 20 Hz.

3. Data Processing

A laptop computer controls the sensor. The operating program was developed with MATLAB 7.2 software. The program was converted to a standalone application using the MATLAB compiler. It performs the following tasks at periodic time intervals:

- connection to the weather transmitter WXT510 to acquire the weather parameters (RS232 connection);
- connection to the DT9832 acquisition module with a USB port to record the signals from transmission over the cell and the transmission from the FP interferometer;
- connection to the acquisition National Instruments Daqcard 6036E to record the gas temperature and pressure;
- weather data and *in situ* spectra are collected by the computer.

An example of a recorded spectrum is shown in Fig. 4. The calculated spectrum for the determination of the baseline and the FP etalon signal are also displayed in Fig. 4.

The following operations are performed during data processing:

- Cell path and FP signals are used to perform the wavenumber calibration. The frequency calibration is determined by applying a third-degree polynomial interpolation to the interference fringes in the FP signal. The absolute value of the frequency is known from the position of the CH_4 absorption line in the cell signal.

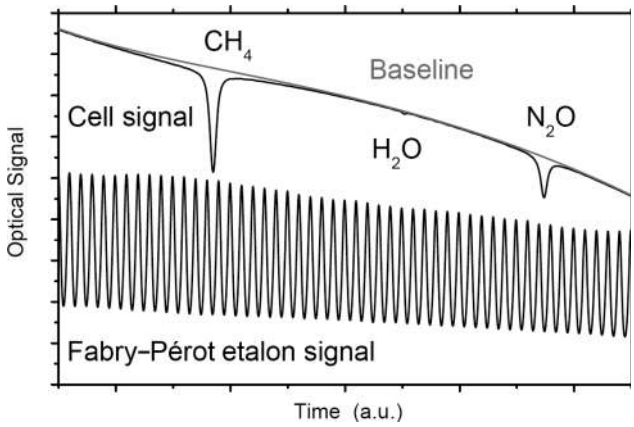

Fig. 4. Average signal of 50 elementary spectra is 0.5 s. The upper black curve shows the signal obtained with 45 mbar of atmospheric air in the cell. The gray curve represents the baseline. The lower curve represents fringes obtained from the 0.01 cm^{-1} free spectral range etalon.

- Baseline correction is a major issue for laser absorption spectrometry. For laboratory measurements we usually determine the baseline by applying a third-degree polynomial interpolation over the full transmission region on both sides of the absorption line. At ground level, under standard conditions and due to the contribution of the open path outside of the cell, there is no full transmission region. The baseline is obtained as follows:

- A synthetic absorption spectrum is calculated using a standard concentration for CH_4, N_2O, and H_2O. This absorption spectrum includes the contribution of the absorption cell and of the open path in the laboratory.
- This synthetic spectrum is used to divide the experimental spectrum to obtain an approximate baseline.
- Finally, a polynomial interpolation on the selected area of the approximate baseline is performed to obtain the final baseline. For the measurements discussed here the selected area are the first 200 points, 300 points in the middle of the spectrum, and the 150 last points. Numerical simulations have been performed to determine which area to select.
- Once the baseline is determined the atmospheric transmission can be extracted from the spectrum. The N_2O and CH_4 volume mixing ratio are finally obtained from the transmission by applying a nonlinear least squares fit to the full molecular line shape using a Voigt model. The small H_2O line inside of the laser scanning range is taken into account in the retrieval process to model the atmospheric transmission and to determine the baseline. During the fitting procedure the N_2O and CH_4 mixing ratio and the position of the lines and the coefficients of the baseline are adjusted.

An example of a recorded spectrum is shown in Fig. 5. The line shape was modeled with a Voigt profile and the resulting residual is also displayed in Fig. 5. The residual features an M shape, which is typical when using the Voigt model approach [16]. The fitting can be improved and the residual reduced by using profiles such as the Rautian–Sobel'man [17] or Galatry [18] line shape functions. However the residual with the Voigt profile is $< 1\%$. Moreover the use of more complicated profiles would increase the processing time with no significant improvement in the accuracy of the concentration retrieval [19].

4. Performance of the Instrument

The precision of the instrument may be evaluated showing a zoom on the small H_2O line in the middle of the recorded spectrum in Fig. 5. This zoom is presented in Fig. 6 with the residual obtained after the fitting procedure. One can observe small undesirable

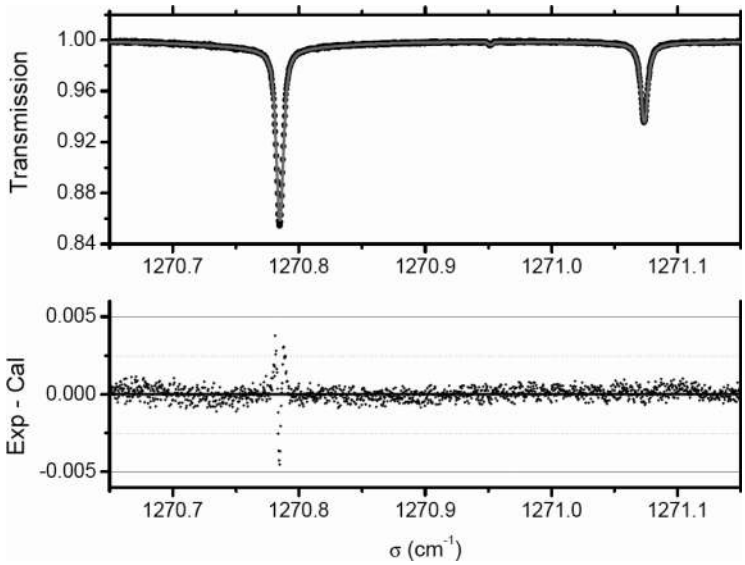

Fig. 5. Example of a recorded spectrum for air (black points) and fitted spectrum (gray curve). The (experimental minus calculated) residual is shown in the lower panel. The retrieved volume mixing ratios are 1.92 ppm of CH_4 and 320 ppb of N_2O.

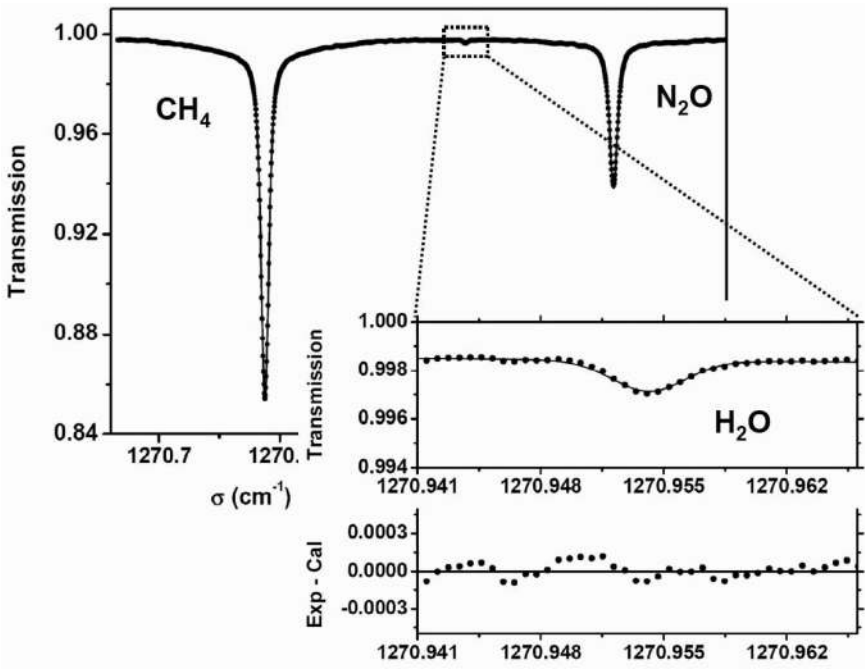

Fig. 6. Zoom spectrum on the small H_2O line at 1270.95 cm^{-1}. The (experimental minus calculated) residual is shown in the lower panel.

fringes due to the multipass system. The estimation of the (experimental minus calculated) residual inside and outside the H_2O line permits determination of an absorption detection limit lower than 2×10^{-4}. This corresponds to a limit of detection of ~1 ppb for N_2O and 2.7 ppb for CH_4. Stability and laboratory tests of the instrument based on the Allan variance method have become a standard procedure for the evaluation of the quality of an instrument [20]. The Allan variance is a very useful tool to detect drifts (i.e., linear or nonlinear slopes superimposed to a signal) and also fringes (i.e., periodic components). We have recorded the time evolution of ambient N_2O concentrations and assumed that the concentration was constant. Thermodynamics parameters were not stabilized. Therefore pressure, temperature, and relative humidity were obtained from the weather sensor. Figure 7 shows a set of concentration data recorded over a period of 7 h and the corresponding Allan variance calculated in [21]. The integration time was 0.5 s per spectrum, and the interval between the two acquisitions was 5 s. The top panel displays the time dependence of the N_2O concentration. The one-sigma standard deviation is 5.7 ppbv. A certain long-term trend of N_2O concentration in this figure, we suspect a long-term trend in the offset of the pressure sensor that we will control more precisely for the next measurement set. The lower panel depicts a log–log plot of the Allan variance versus the integration time (τ) in seconds. The Allan variance decreases and, hence, only the white noise is dominant up to 1280 s integration time. In most practical cases it is very useful to refer to the particular integration time in the Allan variance plot where the minimum occurs. This minimum describes the turnover point, where the white noise in the logarithmic plot becomes dominated by additional and undesired drift noise. The variance minimum at $\tau_{\text{Allan}} = 1280$ s corresponds to a minimum σ_{Allan} of 0.5 ppb; and for CH_4 the variance minimum at $\tau_{\text{Allan}} = 1280$ s corresponds to a minimum σ_{Allan} of 3 ppb. These are the maximum precisions reachable, which satisfy the field measurement requirements asking for sensitivities to flux variability of 1 ppb for N_2O and 10 ppb for CH_4.

5. Measurement of N_2O and CH_4 Concentrations

The instrument has been used to record a series of ambient air measurements. Ambient air samples were collected from outside the laboratory building using a 25 m Teflon tube. The spectrometer was located in the laboratory. A filter was put at the tube entrance to prevent dust entering the optical cell. The vegetation all around the laboratory is mainly a meadow with some oaks. For these measurements the sample gas outside the laboratory was brought from atmospheric pressure to ~40 mbar across the inlet orifice of the new-design multipass 140 m length cell. The system was operated at an air flow of ~5 L min^{-1}. N_2O and CH_4 concentrations have been monitored during a period of 1 day. Figure 8 shows these measurements along with temperature. The mean N_2O volume mixing ratio was ~319 ppb and the mean CH_4 volume mixing ratio was 1.93 ppm, which are typical background troposphere boundary layer values. Over this one-day period, no cycle for N_2O nor CH_4 was observed. Moreover no correlation between concentrations and weather conditions at ground level were observed. This experiment demonstrates the capabilities of the

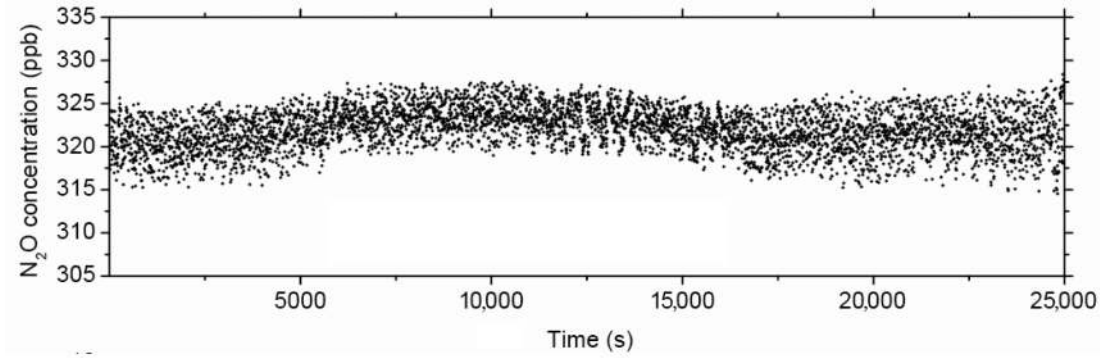

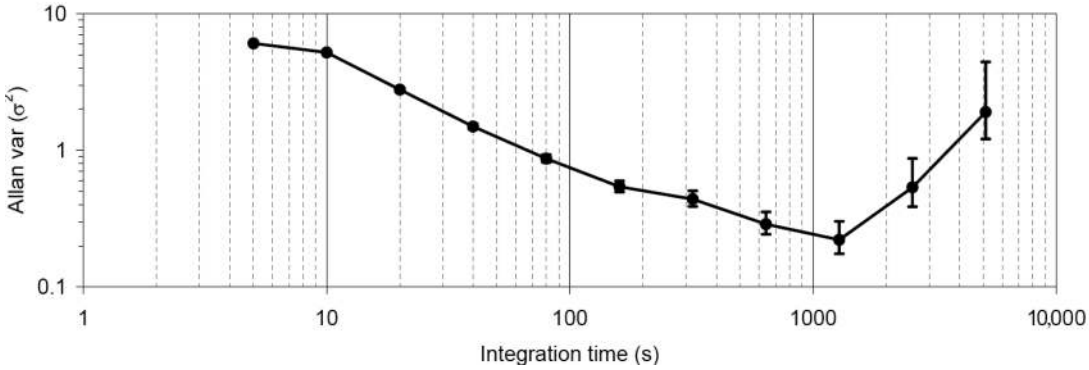

Fig. 7. N_2O concentrations over 7 h and corresponding Allan variance.

developed instrument for a long time online atmospheric accurate measurement.

Added mineral N fertilizer is susceptible to gaseous loss via microbial denitrification, particularly if fertilization is accompanied by irrigation, which creates anaerobic microhabitats suitable for denitrifying bacteria. Denitrification can lead to the release of either N_2 or N_2O as gaseous end products. Thus the study of the time response of N_2O fluxes to a fertilizer addition in a soil sample is of high interest [13]. Each soil sample enriched with ferlilizer was located in a closed chamber with a volume of 10 dm^3. The box containing the soil sample was then connected to the spectrometer using a 1 m length tube made of Teflon and with a diameter of ~5 mm. For this measurement 3.8 g of ammonium nitrate (33% N) were added to the soil sample (mass of 4 kg) that was previously saturated with water (this supply was equivalent to 300 kg of Nha^{-1}). Then N_2O and CH_4 concentrations were monitored during a period of 9 h after the addition of a commercial fertilizer. Figure 9 shows these measurements. The N_2O volume mixing ratio varies from 320 ppb up to > 800 ppb after 9 h. The CH_4 volume mixing ratio remains constant at ~1.93 ppm. This second experiment also demonstrates the capabilities of the developed instrument for rapid measurements and sensitivity to flux variability.

Finally the instrument was successfully used to compare the response of six different soil samples to the addition of N fertilizer. The six soils were sampled at a different water content (from 0.27 to 0.59 gg^{-1}). Table 1 presents the results of N_2O and CH_4 obtained concentrations. It is interesting to note that there is no evolution of the CH_4 concentration for the various types of soils, but N_2O concentrations indicate that the various soil samples do not have the same reaction with the addition of N fertilizer. These parameters must be taken into account in the flux model developed by researchers [13].

6. Conclusion

The use of a cutting-edge QCL for atmospheric measurements of N_2O and CH_4 with the purpose of agricultural applications was demonstrated. The performances of the instruments in terms of detection limit, temporal resolution, and inaccuracy in the concentration retrieval is in full compliance with our science objectives. A high power source permits increasing sensitivity for the detection of low gas concentration levels by improving the signal-to-noise ratio of the spectrometer. This also permits the use of thermoelectric cooled detectors rather than cryogenic detectors, greatly facilitating field deployment. In this paper we have presented an experimental setup based on cw DFB QCL technology operating at RT for the simultaneous analysis of N_2O and CH_4 in the Earth's atmosphere. The detection limit and the long-term stability of the instrument were evaluated using the Allan variance technique. The developed instrument has been successfully tested for various preliminary *in situ* measurements. A set of concentration data over a period of 26 h was recorded to demonstrate the capability of the sensor

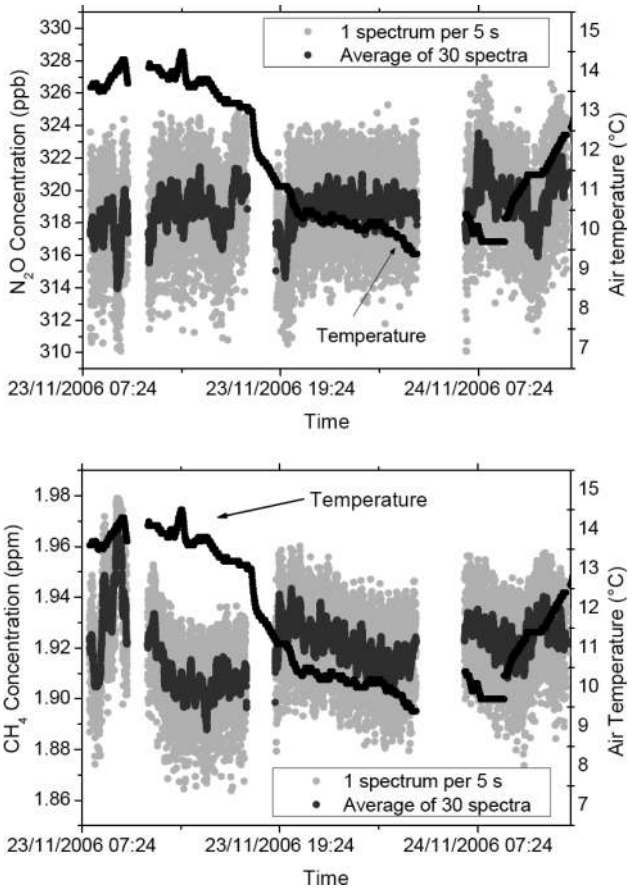

Fig. 8. Atmospheric N_2O (upper panel) and CH_4 (lower panel) measurements. Gray points correspond to concentrations obtained each 5 s and black points correspond to an average on 30 successive results.

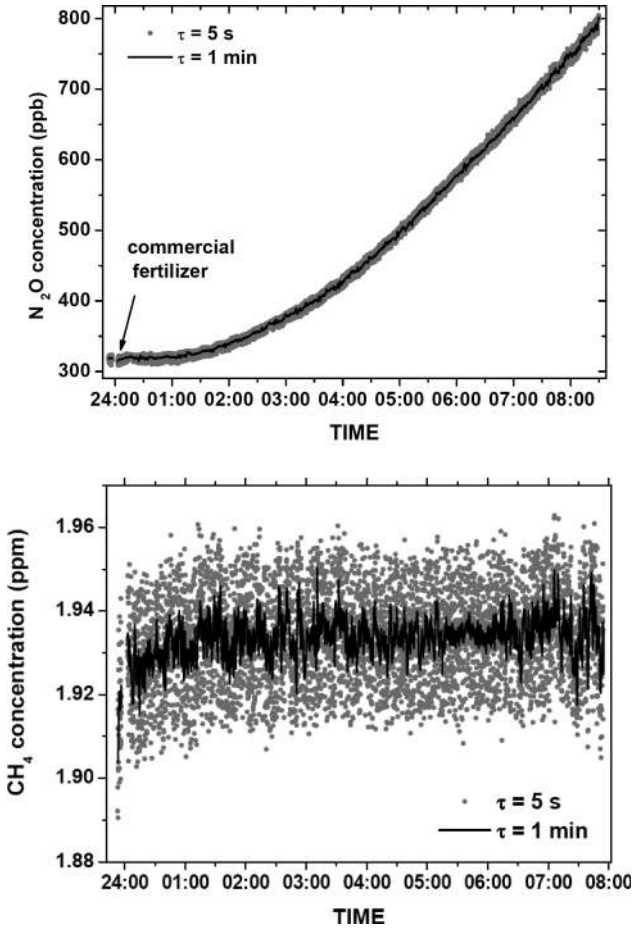

Fig. 9. N_2O (upper panel) and CH_4 (lower panel) concentration measurements after a N fertilizer addition. Gray points correspond to concentrations obtained each 5 s and the black curve corresponds to an integration time of 1 min.

to detect N_2O and CH_4 concentration variations. Moreover the sensor has been applied to study the time response of N_2O fluxes to a fertilizer addition in a soil sample and to compare the response of six different soil samples to this kind of addition. Further developments such as reduction of the cell volume and the use of RT detectors will permit constructing a powerful instrument for the *in situ* measurements of N_2O and CH_4 in the Earth's atmosphere that will be used by the agronomical and biogeochemical communities, for instance for precisely evaluating the impact of agricultural activities on global warming and for evaluating the impact of global warming on CH_4 as a carbon sink in peatlands.

Table 1. N_2O and CH_4 Concentrations for Various Soil Samples After Addition of N Fertilizer

Soil Texture (Soil Type [22])	CH_4 (ppm)	N_2O (ppm)
Reference (ambient air without soil)	1.93 ± 0.02	0.319 ± 0.002
Clay soil (Eutric Fluvisol)	1.92 ± 0.02	54.2 ± 0.6
Clay loam soil (Mollic Fluvisol)	1.94 ± 0.02	81.4 ± 0.9
Humic soil (Mollic Fluvisol)	1.93 ± 0.02	74.8 ± 0.8
Clay loam soil (Haplic Luvisol)	1.93 ± 0.02	66.7 ± 0.7
Clay loam soil (Haplic Luvisol)	1.92 ± 0.02	43.1 ± 0.5
Loamy soil (Gleyic Luvisol)	1.91 ± 0.02	1.52 ± 0.01

References

1. Intergovernmental Panel on Climate Change (IPCC), "*Climate Change 2007: the Physical Science Basis, Summary for Policymakers*," (IPCC, 2007).
2. A. R. Mosier, "Soil processes and global change," Biol. Fertil. Soils **27**, 221–229 (1998).
3. T. Mitsui, M. Miyamura, A. Matsunami, K. Kitagawa, and N. Arai, "Measuring nitrous oxide in exhaled air by gas chromatography and infrared photoacoustic spectrometry," Clin. Chem. **43**, 1993–1995 (1997).
4. R. Knowles, "Denitrification," Microbiol Rev., **46**, 43–70 (1982).
5. J. I. Prosser, *Nitrification* (IRL, 1986).
6. J. M. Duxbury, D. R. Bouldin, R. E. Terry, and R. L. Tate III, "Emission of nitrous oxide from soils," Nature **298**, 462–464 (1982).
7. H. Flessa, R. Ruser, R. Schilling, N. Loftfield, J. C. Munch, E. A. Kaiser, and F. Beese, "N_2O and CH_4 fluxes in potato fields: automated measurement, management effects and temporal variation.," Geoderma **105**, 307–325 (2002).
8. A. F. Bouwman, "Direct emissions of nitrous oxide from agricultural soils," Nutr. Cycling Agroecosyst. **46**, 53–70 (1996).
9. M. S. Zahniser, D. D. Nelson, J. B. McManus, P. L. Kebabian, and D. Lloyd, "Measurement of trace gas fluxes using tunable diode laser spectroscopy," Philos. Trans. R. Soc. London, Ser. A **351**, 371–382 (1995).
10. D. D. Nelson, B. McManus, S. Urbanski, S. Herndon, and M. S. Zahniser, "High precision measurements of atmospheric nitrous oxide and methane using thermoelectrically cooled mid-infrared quantum cascade lasers and detectors," Spectrochim. Acta, Part A **60**, 3325–3335 (2004).
11. S. Wright, G. Duxbury, and N. Langford, "A compact quantum-cascade laser based spectrometer for monitoring the concentrations of methane and nitrous oxide in the troposphere," Appl. Phys. B **85**, 243–249 (2006).
12. M. Beck, D. Hofstetter, T. Aellen, J. Faist, U. Oesterle, M. Ilegems, E. Gini, and H. Melchior, "Continuous wave operation of a mid-infrared semiconductor laser at room temperature," Science **295**, 301–305 (2002).
13. P. Laville, C. Jambert, P. Cellier, and R. Delmas, "Nitrous oxide fluxes from a fertilised maize crop using micrometeorological and chamber methods," Agric. Forest Meteorol. **96**, 19–38 (1999).
14. L. S. Rothman, D. Jacquemart, A. Barbe, D. C. Benner, M. Birk, L. R. Brown, M. R. Carleer, C. Chackerian, Jr., K. Chance, L. H. Coudert, V. Dana, V. M. Devi, J.-M. Flaud, R. R. Gamache, A. Goldman, J.-M. Hartmann, K. W. Jucks, A. G. Maki, J.-Y. Mandin, S. T. Massie, J. Orphal, A. Perrin, C. P. Rinsland, M. A. H. Smith, J. Tennyson, R. N. Tolchenov, R. A. Toth, J. V. Auwera, P. Varanasi, and G. Wagner, "The HITRAN 2004 molecular spectroscopic database," J. Quant. Spectrosc. Radiat. Transf. **96**, 139–204 (2005).
15. C. Robert, "Simple, stable, and compact multiple-reflection optical cell for very long optical paths," Appl. Opt. **46**, 5408–5418 (2007).
16. V. Zéninari, B. Parvitte, L. Joly, T. Le Barbu, N. Amarouche, and G. Durry, "Laboratory spectroscopic calibration of infrared tunable laser spectrometers for the *in situ* sensing of the Earth and Martian atmospheres," Appl. Phys. B **85**, 265–272 (2006).
17. S. G. Rautian and I. I. Sobel'man, Sov. Phys. Usp. **9**, 701–716 (1967).
18. L. Galatry, "Simultaneous effect of Doppler and foreign gas broadening on spectral lines," Phys. Rev. **122**, 1218–1223 (1961).
19. G. Durry, V. Zéninari, B. Parvitte, T. Le Barbu, F. Lefevre, J. Ovarlez, and R. R. Gamache, "Pressure-broadening coefficients and line strengths of H_2O near $1.39\,\mu$m: application to the *in situ* sensing of the middle atmosphere with balloon-borne diode lasers," J. Quant. Spectrosc. Radiat. Transf. **94**, 387–403 (2005).
20. P. Werle, R. Muecke, and F. Slemr, "The limits of signal averaging in atmospheric trace gas monitoring by tunable diode-laser absorption spectroscopy," Appl. Phys. B **57**, 131–139 (1993).
21. E. S. Ferre-Pikal, J. R. Vig, J. C. Camparo, L. S. Cutler, L. Maleki, W. J. Riley, S. R. Stein, C. Thomas, F. L. Walls, and J. D. White, "Draft revision of IEEE STD 1139–1988 standard definitions of physical quantities for fundamental frequency and time metrology—random instabilities," in *Proceedings of the Annual IEEE International Frequency Control Symposium* (IEEE, 1997), pp. 338–357.
22. ISSS-ISRIC-FAO, "World reference base for soil resources," Rep. No. 84 (World Soil Resources, 1998).